Available online at www.sciencedirect.com

ScienceDirect

Mendeleev Commun., 2022, **32**, 757–758

Mendeleev Communications

Bismuth iron tungstate pyrochlore thin films for photovoltaic applications

Sergey S. Kozlov,[a] Anna B. Nikolskaia,*[a] Olga V. Alexeeva,[a] Ekaterina K. Kosareva,[a,b] Oksana V. Almjasheva,[c,d] Viktor V. Gusarov,[c,d] Oleg I. Shevaleevskiy[a] and Liudmila L. Larina[a]

[a] *N. M. Emanuel Institute of Biochemical Physics, Russian Academy of Sciences, 119334 Moscow, Russian Federation. E-mail: anickolskaya@mail.ru*
[b] *N. N. Semenov Federal Research Center for Chemical Physics, Russian Academy of Sciences, 119991 Moscow, Russian Federation*
[c] *St. Petersburg State Electrotechnical University 'LETI', 197376 St. Petersburg, Russian Federation*
[d] *Ioffe Institute, 194021 St. Petersburg, Russian Federation*

DOI: 10.1016/j.mencom.2022.11.016

Thin films based on the ternary complex oxide $Bi_{0.50}Fe_{0.4}WO_q$ with a cubic pyrochlore structure were obtained and used for the first time as electron-transport layers in perovskite solar cells. The measured power conversion efficiency was ~ 4 rel% higher than that of state-of-the-art TiO_2-based perovskite solar cells.

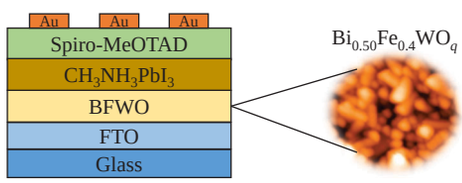

Keywords: pyrochlore, ternary oxide, electron-transport layer, thin film, perovskite solar cells, solar photovoltaics.

Organometallic mixed halide perovskite solar cells (PSCs) have emerged as a promising photovoltaic (PV) technology with the power conversion efficiency (PCE) exceeding 25%.[1–3] A typical PSC consists of a transparent conductive electrode, an electron-transport layer (ETL), a photosensitive perovskite layer, a hole transport material, and a metal electrode.[4,5] The ETL affects the efficiency of electron extraction and hole blocking at the ETL/perovskite interface and provides a significant impact on the PV characteristics and long-term stability of PSCs.[6,7] ETLs should possess a good energy-level alignment with perovskite material and high light transmittance.[8,9] Mesoscopic titanium dioxide layers with the band gap E_g = 3.2 eV are generally used as ETLs.[7] TiO_2-based PSCs demonstrate high PCE, but the performance decreases significantly with time.[10] The PCE degradation in PSCs is attributed to the instability of TiO_2 under UV illumination.[7] A prolonged exposure to sunlight leads to the desorption of oxygen molecules from the TiO_2 layer thus initiating the degradation of the perovskite layer.[11,12] In this regard, the development of novel ETLs with increased irradiance resistance is a major issue in perovskite solar photovoltaics.

Recently, ternary complex oxides attracted much attention due to their excellent electrical and optical properties.[13] These materials are characterized by high electron mobility, high density of active sites, tunable band structures, and high chemical stability under extreme conditions.[7,14] Among them, Bi-containing ternary materials with pyrochlore structure are capable to absorb visible light in short wavelength region, and they can be used as alternative ETLs in PSCs.[15]

In this work, we obtained the ternary complex oxide $Bi_{0.50}Fe_{0.4}WO_q$ (BFWO) by hydrothermal synthesis at pH 2. The BFWO material was used to fabricate ETLs for PSCs. A comparative analysis of the PV parameters measured for BFWO-based PSCs and state-of-the-art PSCs with TiO_2 ETLs demonstrated a new approach to develop efficient PV devices with low degradation of PV parameters under continuous illumination.

BFWO nanopowder with an average particle size of 31 nm was obtained *via* hydrothermal synthesis.[16] Acidic solutions of $Bi(NO_3)_3$ and $Fe(NO_3)_3$·were mixed with an aqueous solution of Na_2WO_4 with continuous stirring and a 4 M solution of NaOH was added dropwise to the resulting suspension to reach pH 2; the mixture was autoclaved at 200 °C for 24 h. The obtained precipitate was separated from the mother liquor by centrifugation, rinsed with distilled water, and dried at 80 °C in air for 20 h. The composition and the pyrochlore structure of the BFWO nanopowder were described previously.[16]

Figure 1 shows the diffuse reflectance spectrum of the BFWO nanopowder. The optical band gap E_g = 2.60 eV was calculated from diffuse reflectance data after the Kubelka–Munk conversion and Tauc plot treatment for indirect transition.[17] This result indicates that the BFWO possesses a narrower band gap and higher visible-light absorption in comparison with TiO_2 particles (3.2 eV). It is well known that the maximum intensity of sunlight reaching the ground corresponds to the yellow-green region of the spectrum (2.1–2.48 eV).[18] Therefore, the BFWO satisfies the condition of efficient conversion of solar power into electrical energy, and it can be successfully used for the development of PSCs.

The BFWO ETLs were fabricated on the surface of FTO conductive glasses by spin coating of a thick paste made by mixing BFWO nanopowder with organic binders (acetic acid, terpineol, and ethyl cellulose) in ethanol followed by annealing at 500 °C in air for 1 h. Figure 2 shows an AFM image of the

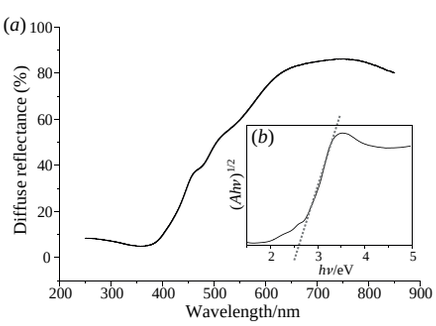

Figure 1 (*a*) Diffuse reflectance spectrum and (*b*) Tauc plot for the BFWO nanopowder.

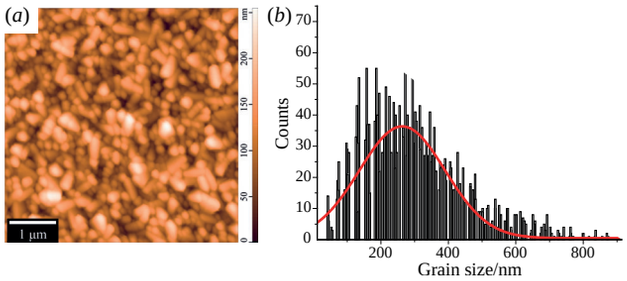

Figure 2 (*a*) AFM image and (*b*) grain size distribution for the BFWO thin film deposited on FTO conductive glass.

BFWO thin film surface. BFWO nanoparticles in a layer tend to form cubic shaped grains with an average size of 228 ± 9 nm. The BFWO films showed good adhesion to the FTO surface and formed a uniform and dense structure, which is an important point for providing the perfect deposition of a perovskite material in order to reduce the defect density at the ETL/perovskite interface.

The BFWO ETLs were used for fabrication of PSCs with the FTO/BFWO/$CH_3NH_3PbI_3$/Spiro-MeOTAD/Au cell architecture under ambient conditions. The perovskite ($CH_3NH_3PbI_3$) layer was formed on the BFWO thin film surface using a conventional one-step deposition method.[19,20] Next, a layer of Spiro-MeOTAD hole transport material was spin-coated, and the ~50-nm thick Au contacts were deposited by vacuum thermal evaporation. A state-of-the-art PSC based on TiO_2 mesoporous layer with the structure FTO/TiO_2 compact layer/meso-TiO_2/$CH_3NH_3PbI_3$/Spiro-MeOTAD/Au was also prepared.

Figure 3 shows the *J–V* curves recorded under standard illumination (1000 W m^{-2}, AM1.5G) for PSCs with BFWO and TiO_2 ETLs. Table 1 summarizes the PV parameters of the fabricated PSCs including short circuit current densities (J_{SC}), open circuit voltages (V_{OC}), fill factors (FFs) and PCE. PSC based on the BFWO material showed a PCE of 13.3%, which is ~ 4% higher than that of the TiO_2-based state-of-the-art PSC (12.8%). It can be attributed to the more uniform ETL structure with fewer amounts of recombination centers at the BFWO/perovskite interface, as compared with TiO_2/perovskite interface characteristics. Thus, the BFWO material can be used as a prospective ETL alternative for the efficient and stable PSCs.

It should be noted that the *J–V* characteristics of the BFWO-based PSCs were measured by sweeping the voltage from +3 V. Previously, similar results were observed in solar cells based on ferroelectric transition-metal oxides. The effect was explained by the electromigration of charged defects (oxygen vacancies) and switching the ferroelectric polarization.[21] Another advantage of BFWO-based ETLs over conventional TiO_2 layers is the lack of using a compact layer between FTO and ETL due to perfect blocking properties of the BFWO films.

The PV parameters of PSCs with BFWO and TiO_2 ETLs were measured after exposure to continuous standard illumination (AM1.5, 1000 W m^{-2}) during 1, 3 and 6 h (see Table 1). The results demonstrate a more stable behavior of the PSCs with

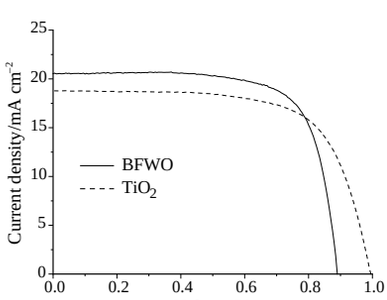

Figure 3 *J–V* curves for the PSCs based on different ETLs.

Table 1 PV characteristics of the PSCs with different ETLs.

Type of ETL	J_{SC}/ mA cm^{-2}	V_{OC}/V	FF (%)	PCE (%)	Duration of continuous illumination/h		
					1	3	6
					PCE (%)	PCE (%)	PCE (%)
TiO_2	18.8	1.00	69.11	12.8	12.6	12.3	11.5
BFWO	20.5	0.89	73.24	13.3	13.2	13.0	12.8

BFWO ETLs (degradation by 3.8% during 6 h) in comparison with those based on TiO_2 layers (by 10.2%).

Thus, the ternary complex oxides $Bi_{0.50}Fe_{0.4}WO_q$ with a cubic pyrochlore structure revealed perfect applicability as ETLs for highly efficient PSCs with improved stability. This class of inorganic materials exhibited intense visible-light absorption and better degradation resistance under continuous UV illumination compared with that of state-of-the-art ETL materials. PCE values for $Bi_{0.50}Fe_{0.4}WO_q$-based PSCs were ~ 4% higher than those obtained for TiO_2-based devices. Taking into account the possibility of tuning the optical and electrical characteristics of Bi-containing ternary pyrochlore materials by changing the pH of hydrothermal fluid during synthesis, we believe that the PV characteristics of PSCs based on them can be further improved.

This work was supported by the Russian Science Foundation (RSF), grant no. 20-69-47124.

Online Supplementary Materials

Supplementary data associated with this article can be found in the online version at doi: 10.1016/j.mencom.2022.11.016.

References

1 M. Green, E. Dunlop, J. Hohl-Ebinger, M. Yoshita, N. Kopidakis and X. Hao, *Prog. Photovolt. Res. Appl.*, 2021, **29**, 3.
2 Y. Li, H. Xie, E. L. Lim, A. Hagfeldt and D. Bi, *Adv. Energy Mater.*, 2022, **12**, 2102730.
3 V. A. Kabanova, O. L. Gribkova, A. R. Tameev and A. A. Nekrasov, *Mendeleev Commun.*, 2021, **31**, 454.
4 P. Basumatary and P. Agarwal, *Mater. Res. Bull.*, 2022, **149**, 111700.
5 A. Yu. Grishko, E. A. Zharenova, E. A. Goodilin and A. B. Tarasov, *Mendeleev Commun.*, 2021, **31**, 163.
6 M. F. M. Noh, C. H.Teh, R. Daik, E. L. Lim, C. C. Yap, M. A. Ibrahim, N. A. Ludin, A. R. M. Yusoff, J. Jange and M. A. M. Teridi, *J. Mater. Chem. C*, 2018, **6**, 682.
7 S. Foo, M. Thambidurai, P. S. Kumar, R. Yuvakkumar, Y. Huang and C. Dang, *Int. J. Energy Res.*, 2022, **46**, https://doi.org/10.1002/er.7958.
8 K. Wang, S. Olthof, W. S. Subhani, X. Jiang, Y. Cao, L. Duan, H. Wang, M. Du and S. Liu, *Nano Energy*, 2020, **68**, 104289.
9 L. Lin, T. W. Jones, T. C.-J. Yang, N. W. Duffy, J. Li, L. Zhao, B. Chi, X. Wang and G. J. Wilson, *Adv. Funct. Mater.*, 2021, **31**, 2008300.
10 R. Liu, L. Wang, Y. Fan, Z. Li and S. Pang, *RSC Adv.*, 2020, **10**, 11551.
11 L. Huang and Z. Ge, *Adv. Energy Mater.*, 2019, **9**, 1900248.
12 P. Roy, N. K. Sinha, S. Tiwari and A. Khare, *Sol. Energy*, 2020, **198**, 665.
13 Y. Zhou, X. Li and H. Lin, *Small*, 2020, **16**, 1902579.
14 M. Thambidurai, F. Shini, P. C. Harikesh, N. Mathews and C. Dang, *J. Power Sources*, 2020, **448**, 2273621.
15 M. Bencina, M. Valant, M. W. Pitcher and M. Fanetti, *Nanoscale*, 2014, **6**, 745.
16 M. S. Lomakin, O. V. Proskurina, A. A. Sergeev, I. V. Buryanenko, V. G. Semenov, S. S. Voznesenskiy and V. V. Gusarov, *J. Alloys Compd.*, 2021, **889**, 161598.
17 J. Tauc, R. Grigorovici and A. Vancu, *Phys. Status Solidi*, 1966, **15**, 627.
18 V. V. Kislyuk and O. P. Dimitriev, *J. Nanosci. Nanotechnol.*, 2008, **8**, 131.
19 M. F. Vildanova, A. B. Nikolskaia, S. S. Kozlov, O. K. Karyagina, L. L. Larina, O. I. Shevaleevskiy, O. V. Almjasheva and V. V. Gusarov, *Dokl. Phys. Chem.*, 2019, **484**, 36.
20 M. F. Vildanova, A. B. Nikolskaia, S. S. Kozlov, O. I. Shevaleevskiy, O. V. Almjasheva and V. V. Gusarov, *Dokl. Phys. Chem.*, 2021, **496**, 13.
21 L. Wang, H. Ma, L. Chang, C. Ma, G. Yuan, J. Wang and T. Wu, *Small*, 2017, **13**, 1602355.

Received: 22nd July 2022; Com. 22/6968